

Thermal Polymerization of Styrene at High Conversions and Temperatures. An Experimental Study

ALBERT W. HUI* AND ARCHIE E. HAMIELEC, *McMaster University, Hamilton, Ontario, Canada*

Synopsis

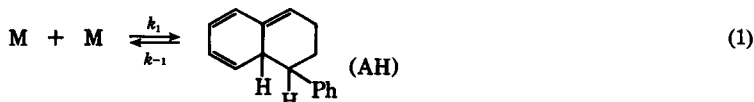
An experimental study of thermal polymerization of styrene in the temperature range 100–200°C and conversion range 0–100% is reported. Conversions, molecular weight averages, and molecular weight distributions were measured. A kinetic model with third-order initiation gives a satisfactory fit of conversion and number- and weight-average molecular weights over the ranges of temperature and conversion investigated. This model should find use in the design, simulation, and optimization of polystyrene reactors.

INTRODUCTION

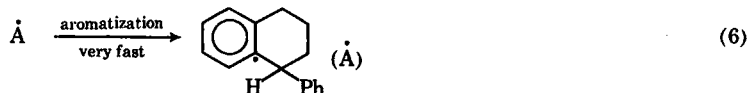
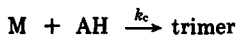
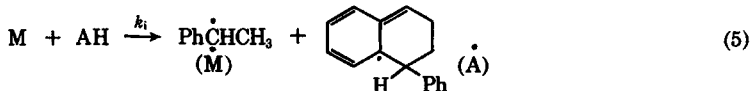
Uninhibited styrene polymerizes even at room temperature, although slowly. Industrial thermal processes usually operate in the temperature range 100–200°C. A comprehensive experimental investigation of the thermal polymerization of styrene over this temperature range and up to high conversions has so far not been reported in the literature. This investigation was initiated to provide this information, in a form suitable for design, simulation, and optimization of polymer reactors.

Many theories have been proposed to account for the unusually high thermal initiation of styrene. Pryor and Lasswell¹ and Pryor and Coco² have reviewed the chronologic development of these theories and have outlined an acceptable mechanism after Mayo for the thermal polymerization of styrene, as follows:

Initiation:



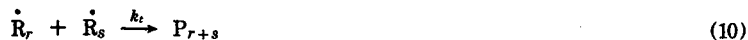
* Present address: Chinook Chemicals Corp. Ltd., 11 King St. West, Toronto, Canada.



Propagation:



Termination by Combination:



Chain Transfer:



In the above scheme, AH is a Diels-Alder adduct and S is a radical scavenger. It was also suggested that AH acts as a transfer agent, with transfer to monomer being of minor importance.

In the development of our empirical model for the thermal polymerization of styrene in bulk over the temperature range, 100–200°C, we will use the above mechanism with two limiting forms of initiation. We have no evidence to suggest that termination by combination operates exclusively at these high temperatures. The use of combination and disproportionation simultaneously would, no doubt, have permitted an equally good fit of our molecular weight data.

THEORY

Let I be the initiation rate in g-moles $\dot{\text{R}}_1/\text{cm}^3 \text{ sec}$;

$$\therefore I = (k_A[\text{A}] + k_B[\dot{\text{M}}])[M] \quad (13)$$

Applying the stationary-state hypothesis to $\dot{\text{A}}$ and $\dot{\text{M}}$,

$$[\dot{\text{A}}] = \frac{k_i}{k_A} [\text{AH}] \quad (14)$$

and

$$\dot{M} = \frac{k_i}{k_B} [AH] \quad (15)$$

$$\therefore I = 2k_i[AH][M]. \quad (16)$$

Applying the stationary-state hypothesis to AH,

$$[AH] = \frac{k_1[M]^2}{k_{-1} + (k_i + k_c)[M] + k_{fAH}\left(\frac{I}{k_i}\right)^{1/2}} \quad (17)$$

$$\therefore I = \frac{2k_1k_i[M]^3}{k_{-1} + (k_i + k_c)[M] + k_{fAH}\left(\frac{I}{k_i}\right)^{1/2}}. \quad (18)$$

We now consider limiting cases of this initiation rate expression.

Initiation Second Order in Monomer

Consider the limit where

$$(k_i + k_c)[M] \gg k_{-1} + k_{fAH}\left(\frac{I}{k_i}\right)^{1/2}$$

$$\therefore I = \left(\frac{2k_1k_i}{k_i + k_c}\right)[M]^2 = 2\bar{k}_1[M]^2. \quad (19)$$

Initiation Third Order in Monomer

Consider the limit where

$$(k_{-1} \gg (k_i + k_c)[M] + k_{fAH}\left(\frac{I}{k_i}\right)^{1/2})$$

$$\therefore I = \left(\frac{2k_1k_i}{k_{-1}}\right)[M]^3 = 2\bar{k}_i[M]^3. \quad (20)$$

In the original fitting of our experimental data, we considered transfer to monomer and neglected transfer to AH. We later considered transfer to AH and neglected transfer to monomer. We also neglect consumption of monomer in reaction (2) and consumption of AH in reaction (4).

MODEL DEVELOPMENT

A considerable volume change is involved in the polymerization of styrene.³ Volume change is accounted for with the use of the variable-volume equation,

$$\begin{aligned} \text{rate} &= \frac{1}{V} \frac{dN}{dt} = \frac{1}{V} \frac{d}{dt} CV \\ &= \frac{dC}{dt} + \frac{C}{V} \frac{dV}{dt} \end{aligned} \quad (21)$$

where C is the concentration of any species.

A linear relationship of volume versus the conversion of monomer was used, i.e.,

$$V = V_0(1 + \epsilon X) \quad (22)$$

and

$$\frac{dV}{dt} = - \left(\frac{V_0 \epsilon}{[M]_0 + \epsilon[M]} \right) + \frac{\epsilon([M]_0 - [M])}{([M]_0 + \epsilon[M])} \frac{d[M]}{dt} \quad (22a)$$

$$\frac{1}{V} \frac{dV}{dt} = - \left(\frac{\epsilon}{[M]_0 + \epsilon[M]} \right) \frac{d[M]}{dt} \quad (22b)$$

where ϵ is defined as

$$\epsilon = \frac{V_{X=1} - V_{X=0}}{V_{X=0}}, \quad (23)$$

being the fractional change in volume of the system between zero and complete conversion. Conversion X is defined as the fractional weight of monomer converted,

$$X = \frac{[M]_0 V_0 - [M]V}{[M]_0 V_0} \quad (24)$$

This is combined with eq. (22) to give

$$X = \frac{[M]_0 - [M]}{[M]_0 + [M]\epsilon} \quad (25)$$

For the suggested kinetic scheme, the moment equations for free radicals and dead polymer species are⁴

$$\begin{aligned} \frac{dGR(s,t)}{dt} = s(1 + k_{fm}[M] GR(1,t)) + GR(s,t) \left[k_p[M](s-1) \right. \\ \left. - k_{fm}[M] - k_t GR(1,t) - \frac{1}{V} \frac{dV}{dt} \right] \end{aligned} \quad (26)$$

$$\frac{dGP(s,t)}{dt} = GR(s,t) \left[k_{fm}[M] + \frac{1}{2} k_t GR(s,t) \right] - \frac{GP(s,t)}{V} \frac{dV}{dt} \quad (27)$$

where

$$GR(s,t) = \sum_{r=1}^{\infty} s^r \dot{R}_r; \quad GP(s,t) = \sum_{r=2}^{\infty} s^r P_r \quad (28)$$

and neglecting consumption in initiation and transfer reactions, the rate equation for monomer may be written as

$$\frac{d[M]}{dt} = - k_p[M] GR(1,t) - \frac{[M]}{V} \frac{dV}{dt} \quad (29)$$

The method of moments has the advantage of reducing the number of ordinary differential equations that need be solved. Further simplifications

can be had by applying the stationary state hypothesis to free-radical equations. This gives

$$\frac{d[M]}{dt} = -R_p - \frac{[M]}{V} \frac{dV}{dt} \quad (29a)$$

$$GR(s,t) = \frac{-sR_p(C_m + \beta)}{k_p[M]\{s - 1 - C_m - R_p^{1/2}\beta\}} \quad (26a)$$

where

$$C_m = \frac{k_{fm}}{k_p} \text{ and } \beta = \frac{k_t R_p}{k_p^2 [M]^2}$$

$$\frac{d(MP)_0}{dt} = R_p [C_m + \beta/2] - \frac{(MP)_0}{V} \frac{dV}{dt} \quad (30)$$

$$\frac{d(MP)_1}{dt} = R_p - \frac{(MP)_1}{V} \frac{dV}{dt} \quad (31)$$

$$\frac{d(MP)_2}{dt} = \frac{R_p}{(C_m + \beta)^2} [2C_m + 3\beta] - \frac{(MP)_2}{V} \frac{dV}{dt} \quad (32)$$

where

$$(MP)_0 = \sum_{r=2}^{\infty} P_r; \quad (MP)_1 = \sum_{r=2}^{\infty} r P_r; \quad (MP)_2 = \sum_{r=2}^{\infty} r^2 P_r.$$

The number- and weight-average chain lengths are

$$r_N = (MP)_1 / (MP)_0 \quad (33)$$

$$r_w = (MP)_2 / (MP)_1 \quad (34)$$

For initial rates, the following algebraic relationships are obtained

$$R_p = \frac{I}{\beta} \quad (35)$$

$$r_N^{-1} = C_m + \beta/2 \quad (36)$$

$$r_w / r_N = 2 \left[1 - \left(\frac{\beta/2}{C_m + \beta} \right)^2 \right] \quad (37)$$

$$[\eta] = \frac{K \bar{M}^a}{(C_m + \beta)^{1+a}} \left[C_m \Gamma(2 + a) + \frac{\beta}{2} (\Gamma(3 + a) - (C_m + \beta) \Gamma(2 + a)) \right] \quad (38)$$

where K and a are Mark-Houwink constants, \bar{M} is monomer molecular weight, and Γ is the gamma function and

$$\Gamma(2 + a) = \int_0^{\infty} \rho^{1+a} \exp(-\rho) d\rho$$

Measurements of R_p , r_N , and r_w are sufficient to determine I , k_{fm}/k_p , and k_i/k_p^2 over the range of conversions studied for a series of isothermal polymerizations. A measurement of intrinsic viscosity could be used in place of one of the molecular weight averages.

The measurement of higher molecular weight averages or the molecular weight distribution (MWD) itself does not permit one to obtain individual rate constants. These additional measurements, however, do provide a consistency test for the proposed kinetic model.

Calculation of the differential molecular weight distribution was done in two ways. The first method involved the solution of the differential equations for dead polymer which follow

$$\frac{dP_r}{dt} = R_p \left((C_m)(C_m + \beta) + \left(\frac{1}{2}\beta\right)(C_m + \beta)^2 r \right) \phi^r - \frac{Pr}{V} \frac{dV}{dt} \quad (39)$$

where

$$\phi = \frac{1}{(1 + C_m + \beta)}$$

Equation (39) was solved for 50 dead polymer species at equal intervals of $\Delta \ln r$. This corresponds to the practice used in gel permeation chromatography of integrating the GPC response to calculate M_n , M_w , and M_z . The second method involved the integration of eq. (40),

$$\frac{dP_r}{d[M]} = \frac{R_p \left(C_m(C_m + \beta) + \frac{1}{2}\beta(C_m + \beta)^2 r \right) \phi^r - \frac{Pr}{V} \frac{dV}{dt}}{-\left(R_p + \frac{[M]}{V} \frac{dV}{dt} \right)} \quad (40)$$

Both methods gave identical results, with the latter requiring somewhat less computer time.

Fitting Measured Conversions and M_n and M_w to Find I , k_{fm}/k_p , and k_i/k_p^2

In fitting the solutions of eqs. (29a), (30), (31), and (32) to experimental measurements of conversion, M_n and M_w , we assume that all rate constants are independent of chain length, but can vary with conversion. If it were found that the rate constants were independent of conversion, this would suggest that the gel effect is not significant. Our experimental initial rate data at the higher temperatures are rather limited. In the model, we have therefore used rate constants for initial conditions obtained from correlations available in the literature.⁵ These correlations follow:

$$(k_p)_0 = 1.051 \times 10^7 \exp(-3557/T) \quad (41)$$

$$(k_{fm})_0 = 2.31 \times 10^6 \exp(-6377/T) \quad \left. \vphantom{(k_{fm})_0} \right\} \text{in l./g-mole sec} \quad (42)$$

$$(k_i)_0 = 1.255 \times 10^9 \exp(-844/T) \quad (43)$$

The subscript 0 means value at zero conversion. Densities of styrene monomer and polymer⁸ used in the model are

$$\left. \begin{aligned} \rho_m &= 924 - 0.918 (T - 273.1) \\ \rho_p &= 1084.8 - 0.605 (T - 273.1) \end{aligned} \right\} \text{in g/l.} \quad (44)$$

The group of parameters

$$A = \left[\frac{I}{k_t/k_p^2} \right]^{1/2} \quad (46)$$

was allowed to vary with conversion as follows,

$$A = A_0 \exp(A_1X + A_2X^2 + A_3X^3), \quad (47)$$

where for any temperature A_0 , A_1 , A_2 , and A_3 are independent of conversion X . These constants are found by fitting the experimental conversion-versus-time curve with the integrated form of eq. (29a). The initial I is then found from A_0 and eqs. (41) and (43). We allow k_{fm}/k_p to vary with conversion as

$$C_m = C_{m_0} + B_1X. \quad (48)$$

We justify the use of a linear variation on the basis that the transfer reaction involves a small molecule. The gel effect should be much less pronounced for transfer than for termination reaction. Considering transfer to AH and neglecting transfer to monomer, the expression used for third-order initiation was

$$\frac{\bar{k}_{fAH}}{k_p} = (C_{m_0} + B_1X) \left(\frac{1 + \epsilon X}{[M]_0(1 - X)} \right) \quad (49)$$

where

$$\bar{k}_{fAH} = \frac{k_1 k_{fAH}}{k_{-1}}$$

and the B_1 has the same value in both eqs. (48) and (49).

At this point we have many alternatives for estimating the model parameters. We could express k_t/k_p^2 as some empirical function of conversion such as

$$\frac{k_t}{k_p^2} = \left(\frac{k_t}{k_p^2} \right)_0 \exp(C_1X + C_2X^2 + C_3X^3) \quad (50)$$

and then search for B_1 , C_1 , C_2 , and C_3 to fit the measured M_n and M_w values. We could then substitute back into eq. (46) and find the variation of initiation I with conversion. Another alternative was to use the limiting forms for I , eqs. (19) and (20), and assume that \bar{k}_1 and \bar{k}_t do not depend upon conversion. We therefore evaluate \bar{k}_1 or \bar{k}_t from A_0 or the initiation rate at zero conversion. Equation (47) then immediately gives us the variation of k_t/k_p^2 with conversion. We are then left with a single-

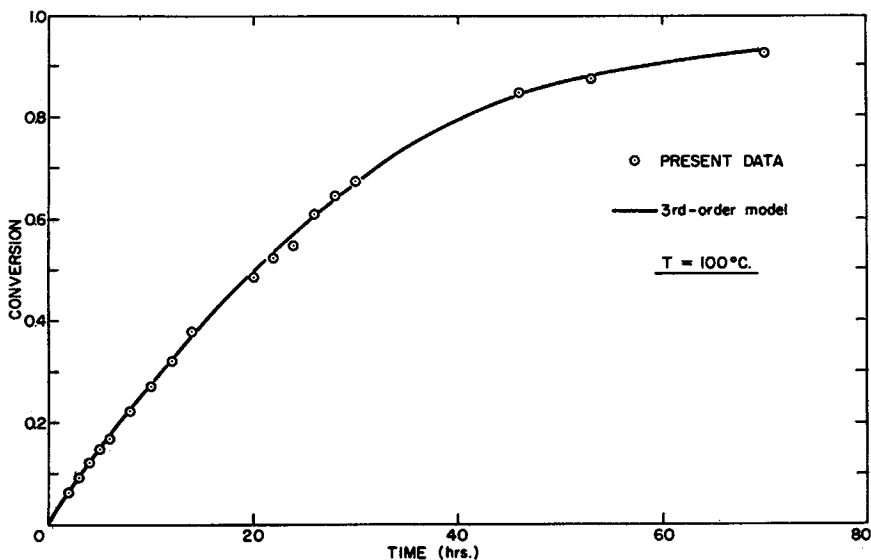


Fig. 1. Experimental conversion-vs.-time data and prediction of third-order model at $T = 100^{\circ}\text{C}$.

variable search for B_1 to fit M_n and M_w . Although the constancy of \bar{k}_1 or \bar{k}_t with conversion may be questioned due to the cage effect at higher conversions, we nevertheless chose the latter alternative. Our conversion data are more accurate than the molecular weight data, and, secondly, the single-variable search gave a reasonable fit of the molecular weights. B_1 was found using a combined fit of M_n and M_w .

The parameters were searched to give the best fit based on the Bayesian criterion.⁶ Very briefly, the proposed model can be represented by

$$Y_{iu} = f_i(x_{iu}^g, \theta_h) + \epsilon_{iu}$$

where f_i are response functions of known form, and θ_h ($h = 1, 2, \dots, m$) are m unknown parameters to be estimated; Y_{iu} ($i = 1, 2, \dots, k$; $u = 1, 2, \dots, n$) are n sets of observations on each of k responses (i.e., measured conversion, and number- and weight-average molecular weights), and x_{iu}^g ($i = 1, 2, \dots, k$; $u = 1, 2, \dots, n$; $g = 1, 2, \dots, r$) are the r variables corresponding to the n sets of observations on each of k responses; ϵ_{iu} represent random errors which are assumed to be normally distributed with mean zero.

The Bayesian criterion of parameter estimation is to choose θ such that the determinant of matrix $[v_{ij}]$ is at a minimum. The element of the matrix $[v_{ij}]$ is defined as

$$v_{ij} = \sum_{u=1}^n \{Y_{iu} - f_i(x_{iu}^g, \theta)\} \{Y_{ju} - f_j(x_{ju}^g, \theta)\}$$

In this case, the problem becomes the search of the parameters until $[v_{ij}]$ is minimum. This was carried out by the Rosenbrock multivariable search routine.

EXPERIMENTAL

Details of all experimental techniques may be found elsewhere.³ Very briefly, thermal polymerization of styrene in bulk was carried out isothermally at 100°, 120°, 140°, 170°, and 200°C in sealed glass ampoules (9, 7, and 5 mm O.D.). Uninhibited styrene (99.73%) was degassed once at 10⁻⁶ mm Hg before use. Conversions up to 95% were measured gravimetrically⁷ and conversion beyond 94%, by UV spectrophotometry.⁹ Molecular weight averages were measured by osmometry and GPC, and molecular weight distributions, by GPC.

A more recent experimental study¹⁰ has provided additional rate data for the thermal polymerization of styrene at temperatures of 160°, 165° and 180°C. These data are used here in addition to the above to test the kinetic model.

RESULTS AND DISCUSSIONS

Model Parameters

Second-order initiation

$$A_0 = 4.23 \times 10^5 \exp(-9936/T) \quad (51a)$$

$$A_1 = 1.99 - 4 \times 10^{-3}T \quad (52a)$$

$$A_2 = 6.62 - 1.25 \times 10^{-2}T \quad (53a)$$

$$A_3 = 1.714 - 4.11 \times 10^{-3}T \quad (54a)$$

$$B_1 = -6.91 \times 10^{-4} \log_{10} \left(\frac{473.1008 - T}{192} \right) \quad (55a)$$

$$\bar{k}_1 = 1.015 \times 10^6 \exp(-13,600/T) \quad (56a)$$

Third-order initiation

$$A_0 = 1.964 \times 10^5 \exp(-10,040/T) \quad (51b)$$

$$A_1 = 2.57 - 5.05 \times 10^{-3}T \quad (52b)$$

$$A_2 = 9.56 - 1.76 \times 10^{-2}T \quad (53b)$$

$$A_3 = -3.03 + 7.85 \times 10^{-3}T \quad (54b)$$

$$B_1 = -1.013 \times 10^{-3} \log_{10} \left(\frac{473.12 - T}{202.5} \right) \quad (55b)$$

$$\bar{k}_1 = 2.19 \times 10^5 \exp(-13,810/T) \quad (56b)$$

where T is in degrees Kelvin, \bar{k}_1 is in l./g-mole sec, and \bar{k}_i is in l.²/g-mole² sec.

In Figures 1, 2, 5, and 7 are shown conversion-versus-time data, both experimental and predicted by the model. These data were used to estimate the parameters A_0 , A_1 , A_2 , and A_3 . Also shown in Figure 7 are

a few experimental points measured by Taherzadeh.¹⁰ In Figures 3, 4, and 6 are shown additional conversion-versus-time data measured by Taherzadeh.¹⁰ These data provide an independent check on the validity of the model for purpose of interpolation at other temperatures. With

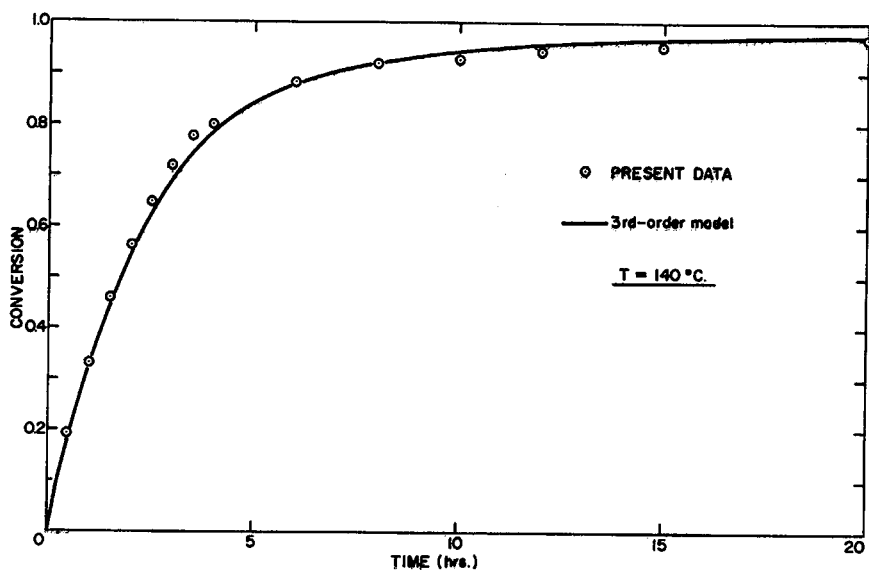


Fig. 2. Experimental conversion-versus-time data and prediction of third-order model at $T = 140^\circ\text{C}$.

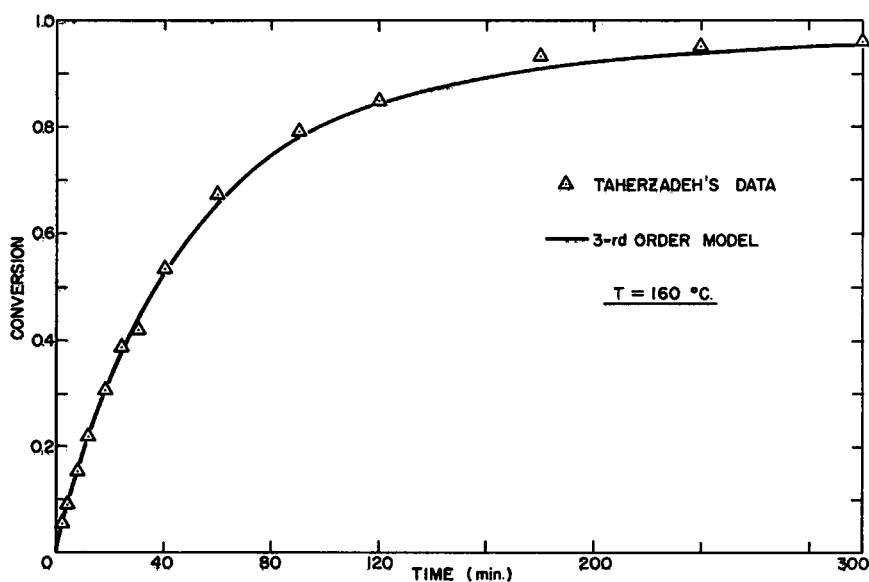


Fig. 3. Experimental conversion-versus-time data and prediction of third-order model at $T = 160^\circ\text{C}$.

some confidence it appears that one can use our model to predict conversion versus time at any temperature in the range 100–200°C.

In Figures 8, 9, 10, and 11 are shown measured and predicted M_n and M_w values. At 100°C, our values of M_w measured by GPC are in excellent

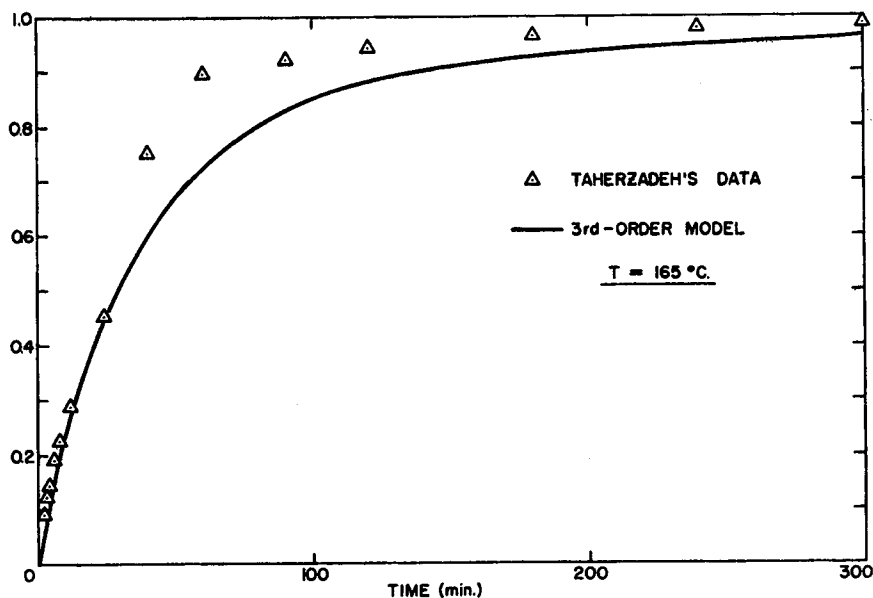


Fig. 4. Experimental conversion-vs.-time data and prediction of third-order model at $T = 165^{\circ}\text{C}$.

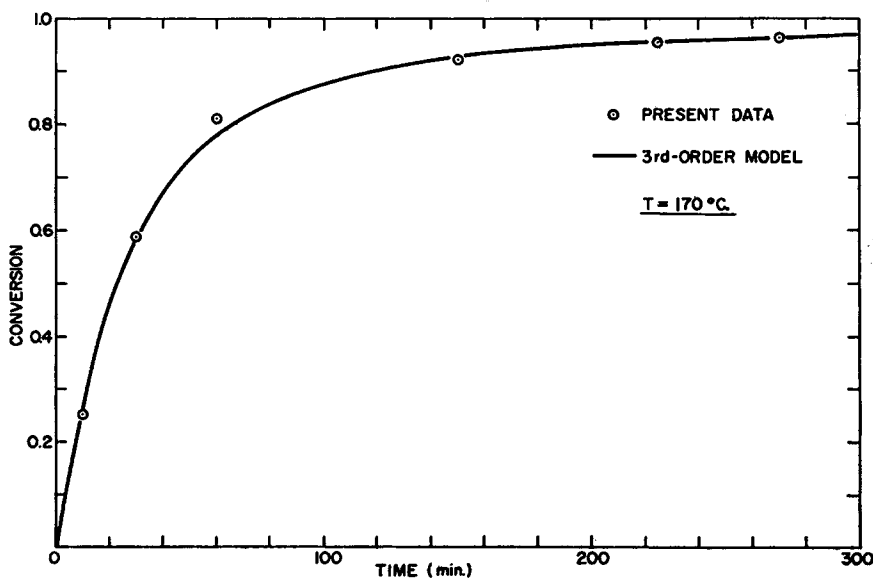


Fig. 5. Experimental conversion-vs.-time data and prediction of third-order model at $T = 170^{\circ}\text{C}$.

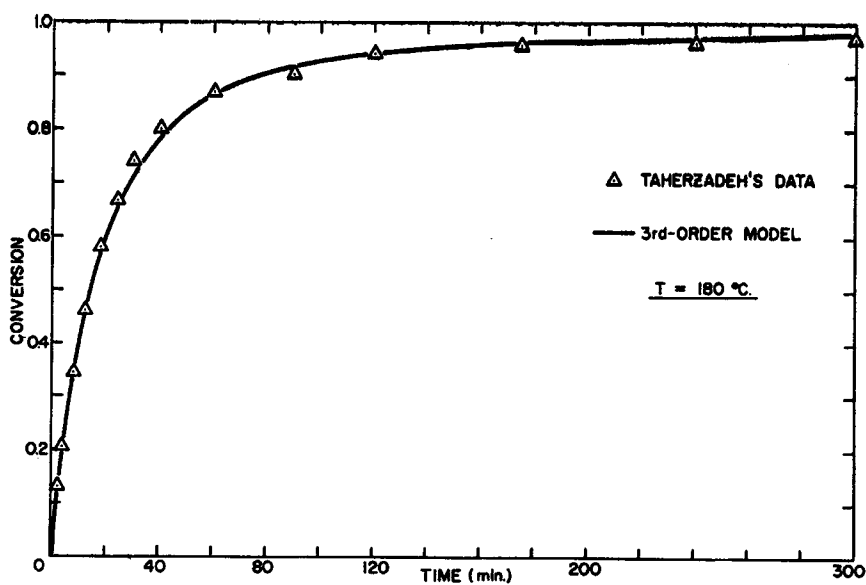


Fig. 6. Experimental conversion vs.-time data and prediction of third-order model at $T = 180^{\circ}\text{C}$.

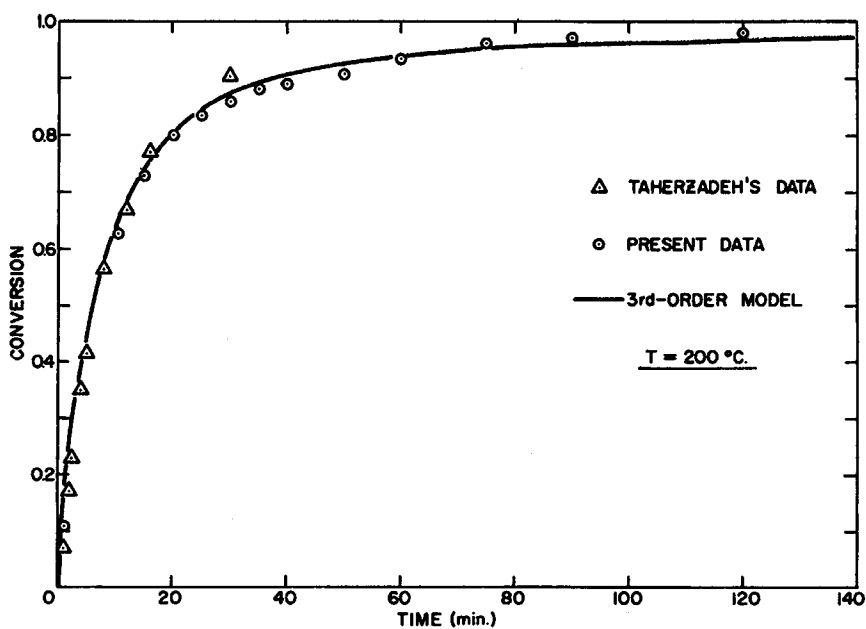


Fig. 7. Experimental conversion-vs.-time data and prediction of third-order model at $T = 200^{\circ}\text{C}$.

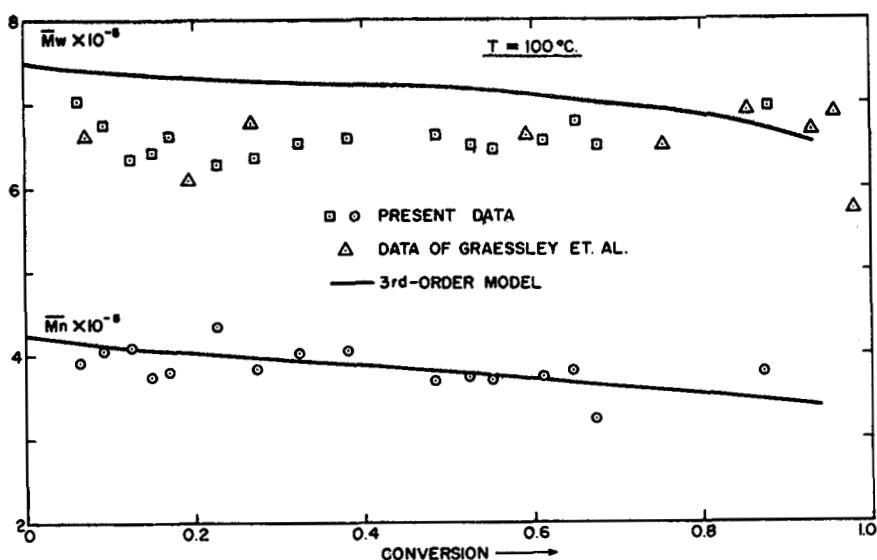


Fig. 8. Experimental number and weight-average molecular weights and prediction of third-order model at $T = 100^\circ\text{C}$.

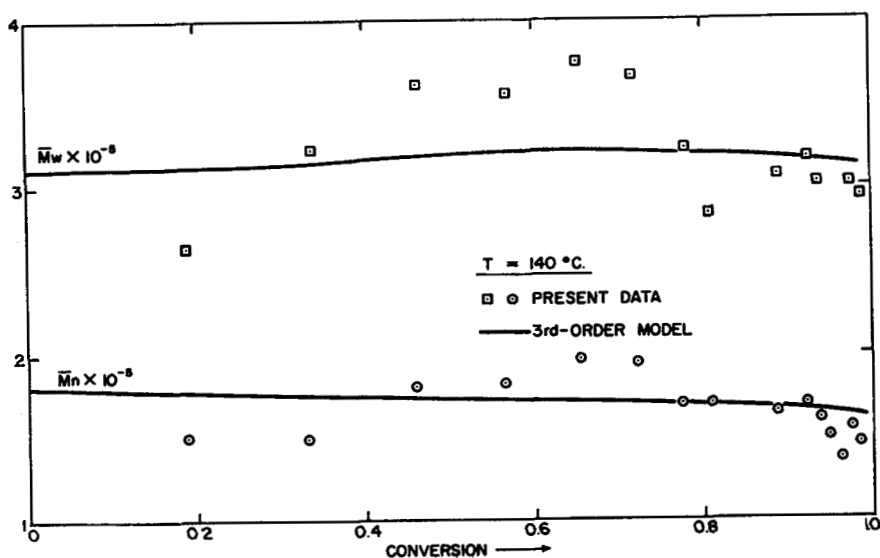


Fig. 9. Experimental number and weight-average molecular weights and prediction of third-order model at $T = 140^\circ\text{C}$.

agreement with those measured by Graessley et al.¹¹ using light scattering. The deviation between model and experimental \bar{M}_w values is quite large. On the other hand, agreement between measured and predicted \bar{M}_w values are satisfactory at 140° , 170° , and 200°C . Measured and predicted \bar{M}_n values are in good agreement at all four temperatures. One would expect a

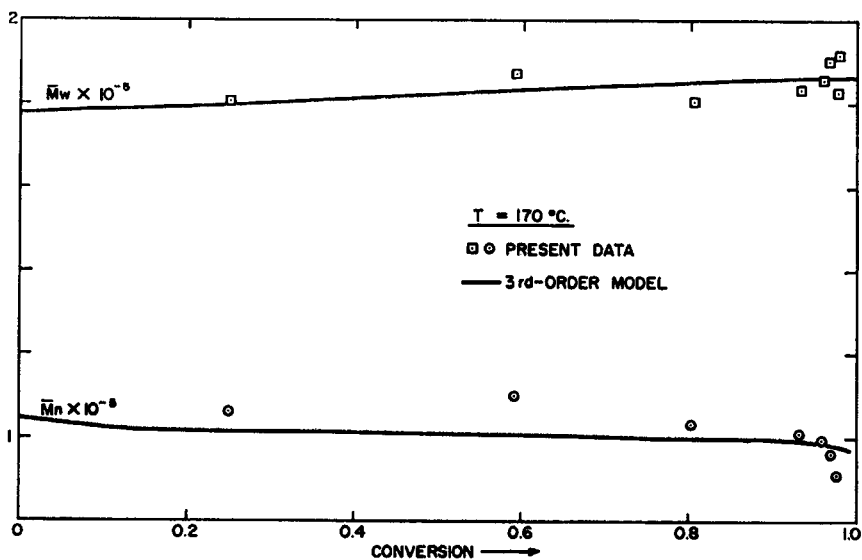


Fig. 10. Experimental number and weight-average molecular weights and prediction of third-order model at $T = 170^\circ\text{C}$.

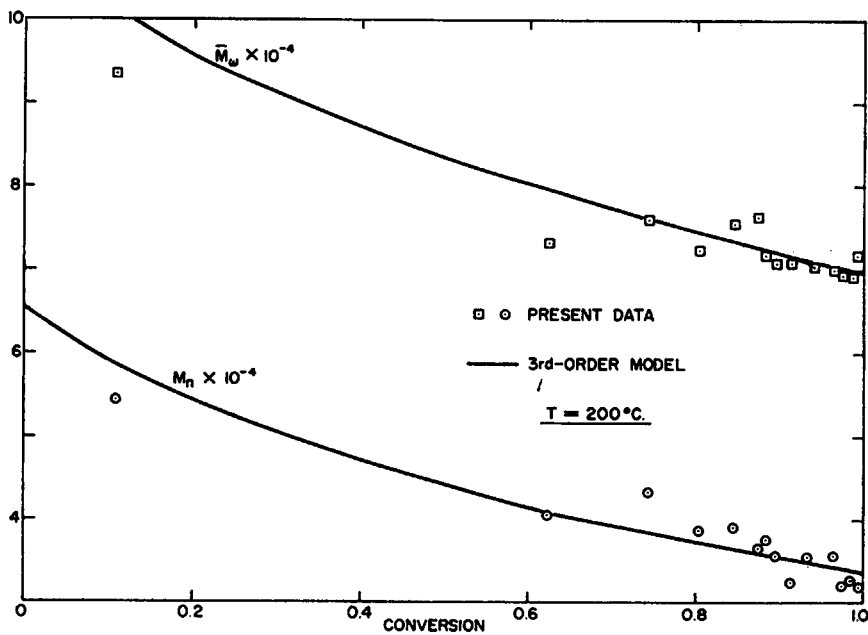


Fig. 11. Experimental number and weight-average molecular weights and prediction of third-order model at $T = 200^\circ\text{C}$.

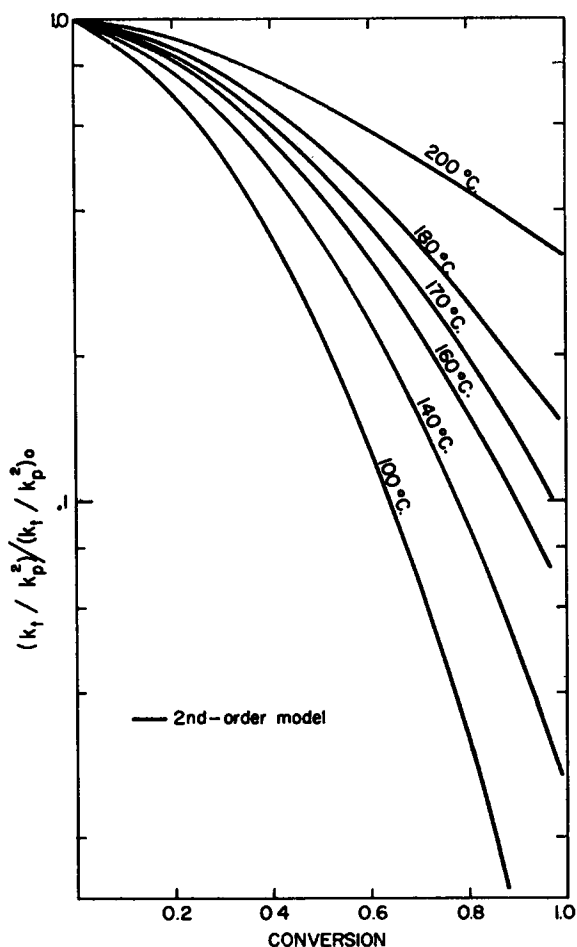


Fig. 12. Variation of k_t/k_p^2 with conversion and temperature for second-order model.

standard deviation in M_n and M_w of about $\pm 10\%$ using GPC at these high molecular weight levels. With this in mind, the fit is probably about as good as can be expected. (It should be remembered that the model is constrained at zero conversion with the use of eqs. (41), (42), and (43).)

To further check the model and the reliability of our GPC measurements, we analyzed certain of the polymer samples by osmometry. These values are listed and compared with GPC values and M_n values calculated from the model in Table I. We further compare the data of Taherzadeh at 165°C and 180°C in Table II with our model. The average molecular weights were measured by GPC. The ampoule sizes used by Taherzadeh were larger than the ones employed in our experimental study, and we feel that disagreement in measured and predicted conversions shown in Table II may be due to significant temperature rise during polymerization in the ampoules at 165°C. The almost opposite behavior at 180° may be due to

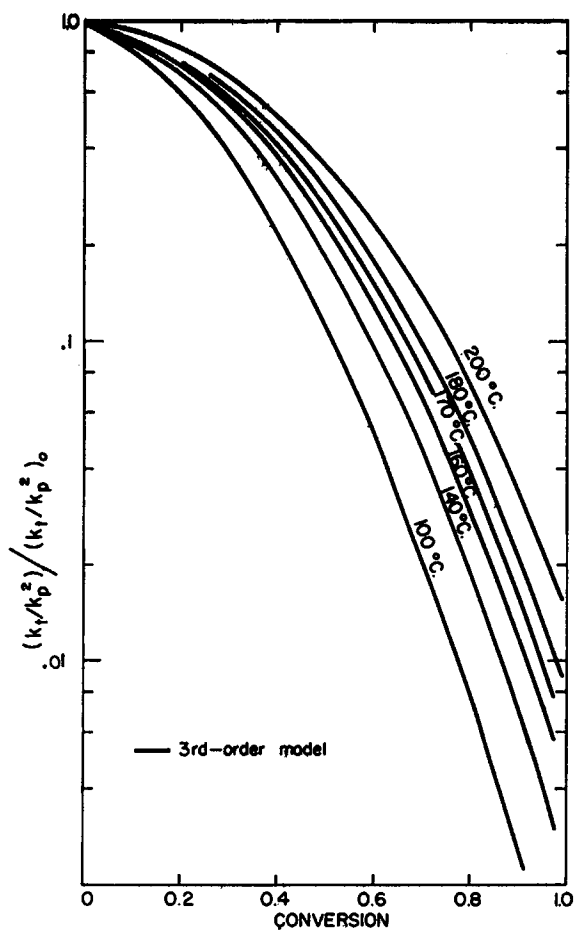


Fig. 13. Variation of k_t/k_p^2 with conversion and temperature for third-order model.

TABLE I
Comparison of Present Experimental Data with Predictions of Model
(Third Order Initiation)

Temp.	X	$M_n(\text{osm})$	$M_n(\text{GPC})$	$M_n(\text{model})$
$T = 100^\circ\text{C}$	0.063	4.16×10^5	3.91×10^5	4.18×10^5
$T = 140^\circ\text{C}$	0.192	1.90×10^6	1.51×10^6	1.76×10^6
	0.653	1.67×10^6	1.96×10^6	1.72×10^6
$T = 170^\circ\text{C}$	0.254	1.00×10^6	1.06×10^6	1.02×10^6
	0.590	1.11×10^6	1.10×10^6	1.01×10^6
	0.965	7.14×10^4	9.10×10^4	9.82×10^4
$T = 200^\circ\text{C}$	0.728	4.62×10^4	4.32×10^4	3.83×10^4
	0.863	4.56×10^4	3.64×10^4	3.58×10^4
	0.992	4.01×10^4	3.50×10^4	3.40×10^4

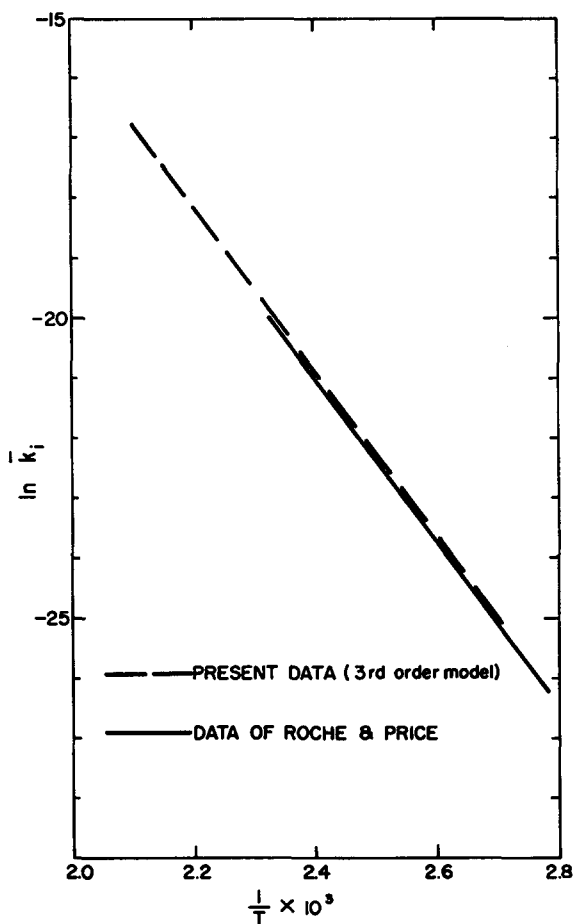


Fig. 14. Temperature dependence of third-order initiation rate constant.

TABLE II
Comparison of Data of Taherzadeh¹⁰ with Predictions of Model
(Third-Order Initiation)

Temp.	X_m	$X(\text{model})$	$M_n(\text{GPC})$	$M_n(\text{model})$	$M_w(\text{GPC})$	$M_w(\text{model})$
$T = 165^\circ\text{C}$	0.286	0.254	1.21×10^5	1.11×10^5	2.16×10^5	1.96×10^5
	0.751	0.603	1.23×10^5	1.10×10^5	2.17×10^5	2.05×10^5
	0.922	0.843	1.24×10^5	1.09×10^5	2.14×10^5	2.05×10^5
	0.984	0.961	1.00×10^5	1.07×10^5	2.01×10^5	2.04×10^5
$T = 180^\circ\text{C}$	0.463	0.435	9.10×10^4	8.50×10^4	1.59×10^5	1.53×10^5
	0.904	0.925	8.10×10^4	8.25×10^4	1.50×10^5	1.56×10^5
	0.971	0.976	7.40×10^4	8.20×10^4	1.45×10^5	1.55×10^5

the induction period required to reach reaction temperature once the ampoule is placed in the temperature bath. The molecular weight averages agree very well. These quantities may be less affected by the aforementioned experimental difficulties.

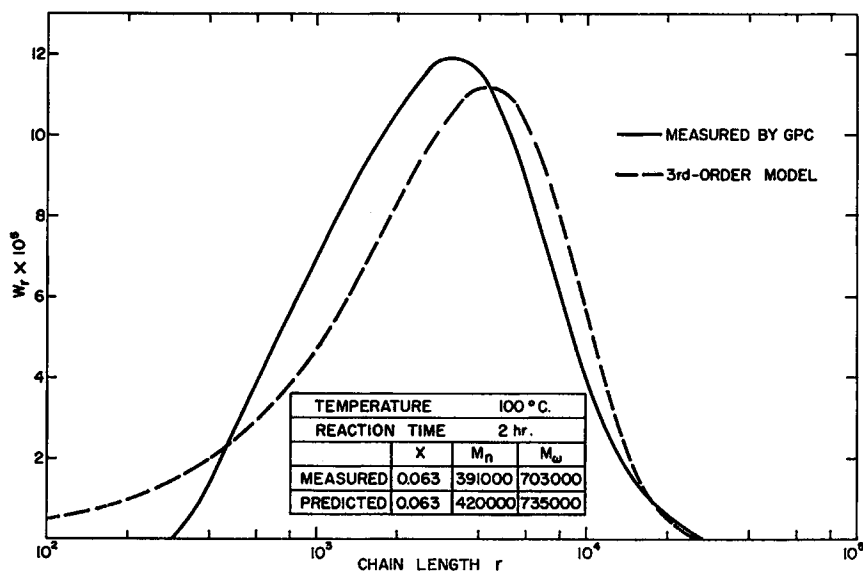


Fig. 15. Molecular weight distribution by GPC and prediction of third-order model at $T = 100^{\circ}\text{C}$.

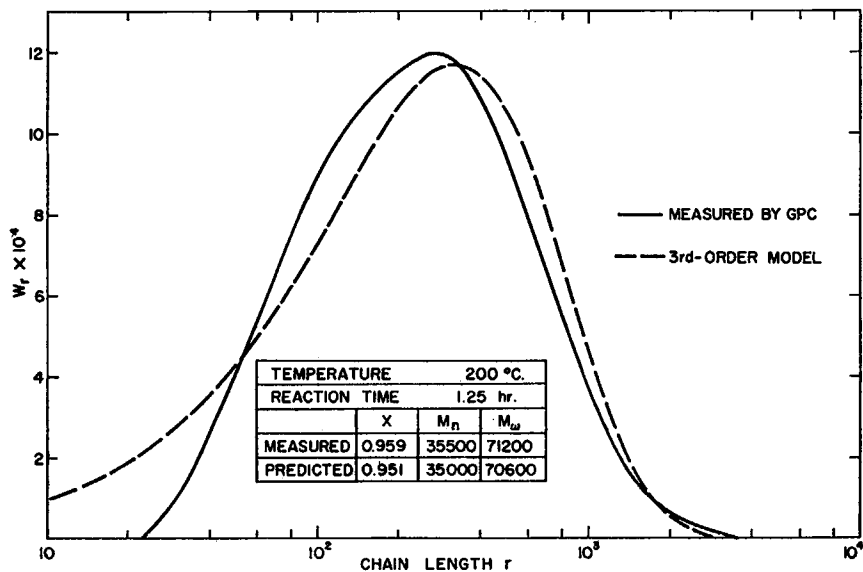


Fig. 16. Molecular weight distribution by GPC and prediction of third-order model at $T = 200^{\circ}\text{C}$.

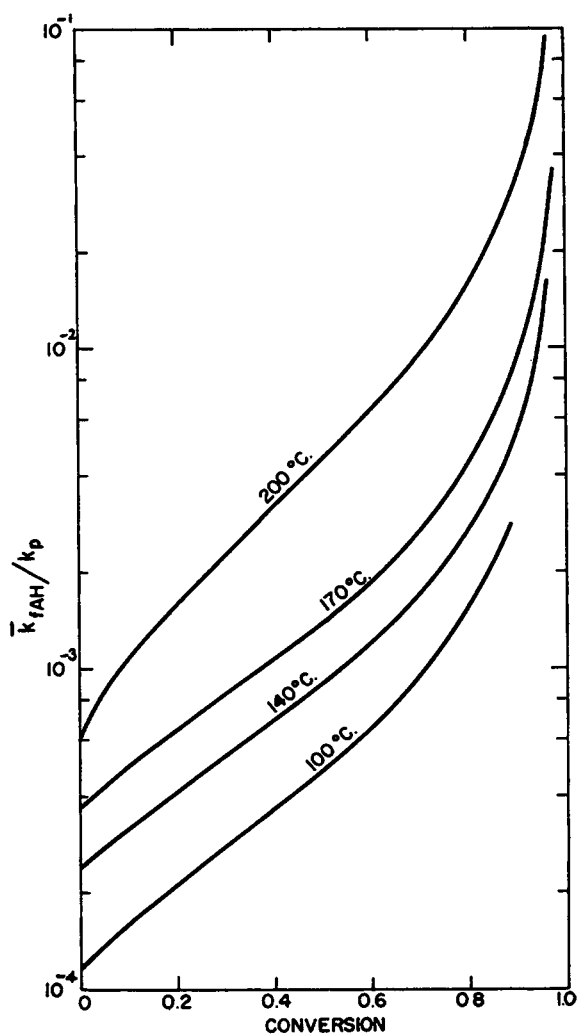


Fig. 17. Variation of \bar{k}_{fAH}/k_p with conversion and temperature for third-order model.

The variation of k_i/k_p^2 with conversion for the second- and third-order models are shown in Figs. 12 and 13. Both models fit the experimental X , M_n , and M_w data equally well. However, we prefer the third-order model on the basis of the more consistent variation of k_i/k_p^2 with temperature and conversion indicated in Fig. 13. In Fig. 14 is shown a comparison of \bar{k}_i measured here with the values measured by Roche and Price.¹² The latter values were corrected for third-order initiation. Duerksen and Hamielec¹³ recently reviewed thermal initiation data for styrene up to 140°C and presented the data of Roche and Price in an Arrhenius plot. These data agree well with most other data in the literature. The agreement of our initiation data for both second- and third-order models with

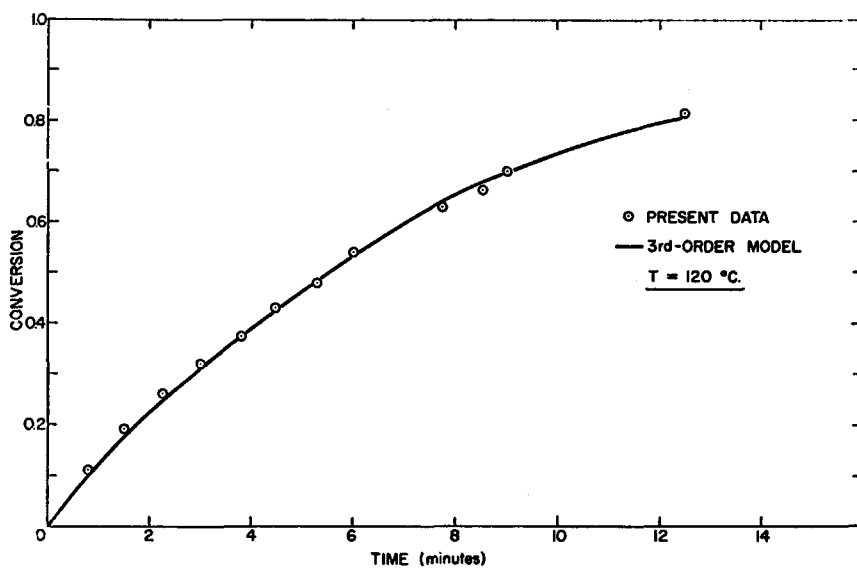


Fig. 18. Experimental conversion-vs.-time data and prediction of third-order model at $T = 120^{\circ}\text{C}$.

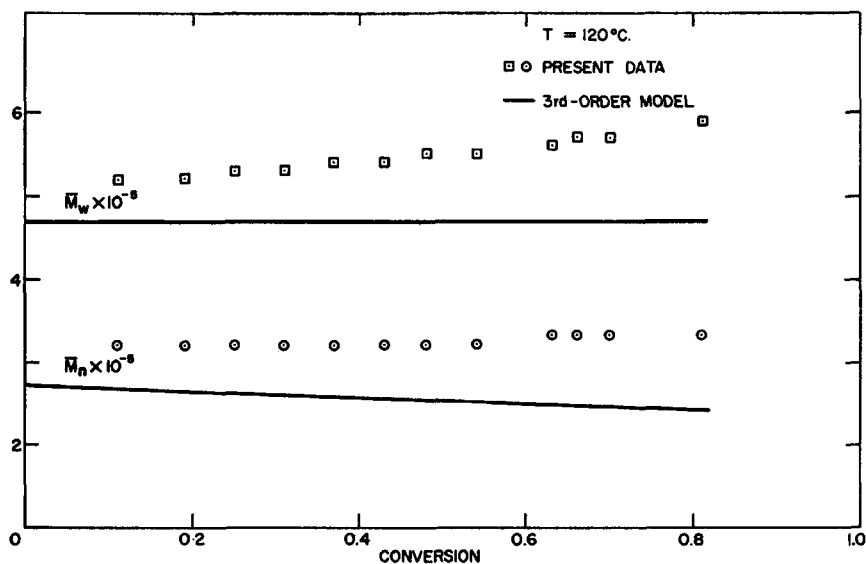


Fig. 19. Experimental number and weight-average molecular weights and predictions of third-order model at $T = 120^{\circ}\text{C}$.

those of Roche and Price is excellent; \bar{k}_t calculated using eq. (56b) is plotted in Fig. 14. Our measured activation energy of 27 kcal is in good agreement with those of other workers.¹³

Examples of typical measured and calculated differential molecular weight distributions are shown in Figs. 15 and 16. The deviations be-

tween measured and predicted distributions are within experimental error. Deviations at the low molecular weight end are probably due to the loss of low molecular weight polymer during precipitation in methanol and dioxane. The model satisfactorily represents the essential features of the polymerization process.

It is of interest to examine transfer to AH and the variation of \bar{k}_{fAH}/k_p with conversion. For third-order initiation, a graph of this variation is shown in Fig. 17. If we assume that \bar{k}_{fAH} is independent of conversion, the variation would be due to a change in the propagation constant k_p with conversion. The decrease in k_p is relatively small compared to the decrease in k_t up to a conversion of about 90%, and then the decrease with conversion is dramatic. This may be partly responsible for the very slow rate of polymerization, and decrease in molecular weight averages near complete conversion.

After the first writing of this paper, we discovered additional data for the thermal polymerization of styrene in our files. These data for 120°C are shown in Figs. 18 and 19. It was obtained using the same experimental techniques.

In summary we have made an experimental study of thermal polymerization of styrene to almost complete conversion and have developed models based on second-order and third-order initiation which should find use in the design, simulation, and optimization of polystyrene reactors. We recommend the use of the third-order models on the basis of the more consistent correlation of the gel effect at high conversions.

The authors are indebted to the National Research Council of Canada, Monsanto Company, Springfield, Mass., U.S.A., and Chinook Chemicals Corporation, Toronto, Ontario, Canada, for financial support of this research project. One of the authors (Albert W. Hui) is indebted to McMaster University for the scholarship provided to make his study possible.

References

1. W. A. Pryor and L. D. Lasswell, *ACS Polymer Preprints*, **11**, 713 (1970).
2. W. A. Pryor and J. H. Coco, *Macromolecules*, **3**, 500 (1970).
3. A. W. T., Hui, Ph.D. Thesis, McMaster University, 1970.
4. W. H. Ray, *Can. J. Chem. Eng.*, **45**, 356 (1967).
5. J. H. Duerksen, A. E. Hamielec, and J. W. Hodgins, *A.I.Ch.E.J.*, **13**, 1081 (1967).
6. G. E. Box, and N. R. Draper, *Biometrika*, **52**, 355 (1965).
7. A. W. T. Hui and A. E. Hamielec, *J. Polym. Sci.*, Part C, No. 25, 167 (1968).
8. W. Patnode and W. J. Scheiber, *J. Amer. Chem. Soc.*, **61**, 3449 (1939).
9. J. Eisenbrand and H. W. Eich, *Z. Anal. Chem.*, **175**, 4 (1960).
10. M. Taherzadeh, M. Eng. Thesis, McMaster University, 1971.
11. W. W. Graessley, W. C. Uy, and A. Gandhi, *Ind. Eng. Chem., Fundam.*, **8**, 696 (1969).
12. R. H. Boundy and R. F. Boyer, *Styrene, Its Polymers, Copolymers and Derivatives*, Rheinhold, New York, 1952, pp. 215-222.
13. J. H. Duerksen and A. E. Hamielec, *ACS Preprints*, Vol. 10, San Francisco, 1969.

Received July 20, 1971

Revised October 26, 1971